

## Potent and Selective Inhibitors of Breast Cancer Resistance Protein (ABCG2) Derived from the *p*-Glycoprotein (ABCB1) Modulator Tariquidar

Matthias Kühnle,<sup>†</sup> Michael Egger,<sup>‡</sup> Christine Müller,<sup>†</sup> Anne Mahringer,<sup>§</sup> Günther Bernhardt,<sup>†</sup> Gert Fricker,<sup>§</sup> Burkhard König,<sup>‡</sup> and Armin Buschauer<sup>\*†</sup>

Department of Pharmaceutical/Medicinal Chemistry II, Institute of Pharmacy, and Institute of Organic Chemistry, Faculty of Chemistry and Pharmacy, University of Regensburg, Universitätsstrasse 31, D-93053 Regensburg, Germany, Institute of Pharmacy and Molecular Biotechnology, University of Heidelberg, Im Neuenheimer Feld 366, D-69120 Heidelberg, Germany

Received November 1, 2008

The efflux pumps ABCB1 (p-gp, MDR1) and ABCG2 (BCRP) are expressed to a high extent by endothelial cells at the blood–brain barrier (BBB) and other barrier tissues and are involved in drug resistance of tumor (stem) cells. Whereas numerous ABCB1 inhibitors are known, only a few ABCG2 modulators with submicromolar activity have been published. Starting from tariquidar (**4**) analogues as ABCB1 modulators, minimal structural modifications resulted in a drastic shift in favor of ABCG2 inhibition. Highest potency was found when the 3,4-dimethoxy-2-(quinoline-3-carboxylamino)benzoyl moiety in **4** was replaced with a 4-methoxycarbonylbenzoyl moiety bearing a hetarylcarboxamido group in 3-position, e.g., quinoline-3-carboxamido (**5**, IC<sub>50</sub>: 119 nM) or quinoline-2-carboxamido (**6**, IC<sub>50</sub>: 60 nM, flow cytometric mitoxantrone efflux assay, topotecan-resistant MCF-7 breast cancer cells); the selectivity for ABCG2 over ABCB1 was about 100–500 fold and the compounds were inactive at ABCC2 (MRP2). Chemosensitivity assays against MCF-7/Topo cells revealed that the nontoxic inhibitor **6** completely reverted ABCG2-mediated topotecan resistance at concentrations > 100 nM, whereas **5** showed ABCG2 independent cytotoxicity. ABCG2 inhibitors might be useful for cancer treatment with respect to reversal of multidrug resistance, overcoming the BBB and targeting of tumor stem cells.

### Introduction

ABC transporters use the energy of ATP-hydrolysis to transport a broad variety of substrates across the cell membrane. These efflux transport proteins include ABCB1 (p-glycoprotein 170, p-gp), ABCC2 (multidrug resistance related protein 2),<sup>1,2</sup> and ABCG2 (BCRP, ABCP<sup>a</sup>, MXR)<sup>3,4</sup> and appear to play a protective role in normal tissues.<sup>5</sup> For example, in the placenta, ABCG2 appears to reduce the passage of substrates from the mother to the fetus and, as reasoned from mice studies,<sup>6</sup> decreases the concentration of certain substrates in the fetal

circulation. A high ABCG2 expression at the luminal surface of the endothelium of microvessel also suggests a tutelary function at the blood–brain barrier. In the therapy of CNS diseases, the aforementioned physiological functions often lead to low drug concentrations in the brain. Numerous anticancer agents are ABCB1 and ABCG2 substrates, which are actively pumped out by the transporters located at the blood–brain barrier. This is one of the primary causes of the failure of chemotherapy in the treatment of malignant brain tumors.<sup>7</sup> Furthermore, ATP-binding cassette (ABC) transporters play a more distinctive role in conjunction with multidrug resistance (MDR). It is estimated that multidrug resistant tumors account for up to half of all cancer-related deaths.<sup>8,9</sup> MDR is caused by the overexpression of efflux transporters such as ABCB1 and ABCG2, located in the plasma membrane of cancer cells, actively extruding a vast number of structurally unrelated compounds, including many commonly used anticancer drugs. Since its discovery in 1998,<sup>10,11</sup> ABCG2 has been the subject of many investigations concerning its role in MDR, and overexpression of the transporter is associated with high-level of resistance to a large number of cytostatics. In addition, ABCG2 transporters have recently attracted interest with respect to a new concept of tumor development and progression, the so-called cancer stem cell hypothesis. The classical stochastic model of tumor development and progression assumes that all cancer cells are tumor initiating and participate in the tumor growth. By contrast, the cancer stem cell concept is based on the idea that only a small side population of cancer cells proliferates, in analogy to the hematopoietic stem cells in the bone marrow. The cells of this side population divide slowly, are capable of long-term self-renewal, and express ABCG2.<sup>12–14</sup> Such cells have been found in numerous established tumor cell lines as well as in tumor biopsies<sup>15–17</sup> and might be responsible for the long-term failure of many cancer chemotherapies. As a

\* To whom correspondence should be addressed. Phone: +49-941 9434827. Fax: +49-941 9434820. E-mail: armin.buschauer@chemie.uni-regensburg.de.

<sup>†</sup> Department of Pharmaceutical/Medicinal Chemistry II, Institute of Pharmacy, Faculty of Chemistry and Pharmacy, University of Regensburg.

<sup>‡</sup> Institute of Organic Chemistry, Faculty of Chemistry and Pharmacy, University of Regensburg.

<sup>§</sup> Institute of Pharmacy and Molecular Biotechnology, University of Heidelberg.

<sup>a</sup> Abbreviations: ABCP, ATP-binding cassette transporter expressed in placenta; aq, aqueous; ATP, adenosine triphosphate; BBB, blood–brain barrier; BCRP, breast cancer resistance protein; Boc, *tert*-Butoxycarbonyl; CDI, 1,1'-carbonyldiimidazole; CNS, central nervous system; DAD, diode array detector; DCM, dichloromethane; DIPEA, diisopropylethylamine; DMAP, 4-dimethylaminopyridine; DMF, dimethylformamide; DMSO, dimethylsulfoxide; EDC, *N*-(3-dimethylaminopropyl)-*N'*-ethylcarbodiimide; EDTA, ethylenediaminetetraacetic acid; EI-MS, electron-impact ionization mass spectrometry; ELSD, evaporative light scattering detection; ES-MS, electrospray ionization mass spectrometry; FACS, fluorescence activated cell sorter; HBTU, (2-(1*H*-benzotriazole-1-yl)-1,1,3,3-tetramethyluronium hexafluorophosphate); HOBt, hydroxybenzotriazole; HR-MS, high resolution mass spectrometry; LSI-MS, liquid-secondary-ion mass spectrometry; MCF-7/Topo cells: human breast cancer cells resistant to topotecan due to overexpression of ABCG2; MDR, multidrug resistance; MRP, multidrug-related protein; MXR, mitoxantrone resistance protein; NOESY, nuclear Overhauser enhancement spectroscopy; p-gp, *p*-glycoprotein; SEM, standard error of the mean; TFA, trifluoroacetic acid; Tf, triflyl, trifluoromethylsulfonyl; THF, tetrahydrofuran; TLC, thin layer chromatography; Tr, trityl, triphenylmethyl.

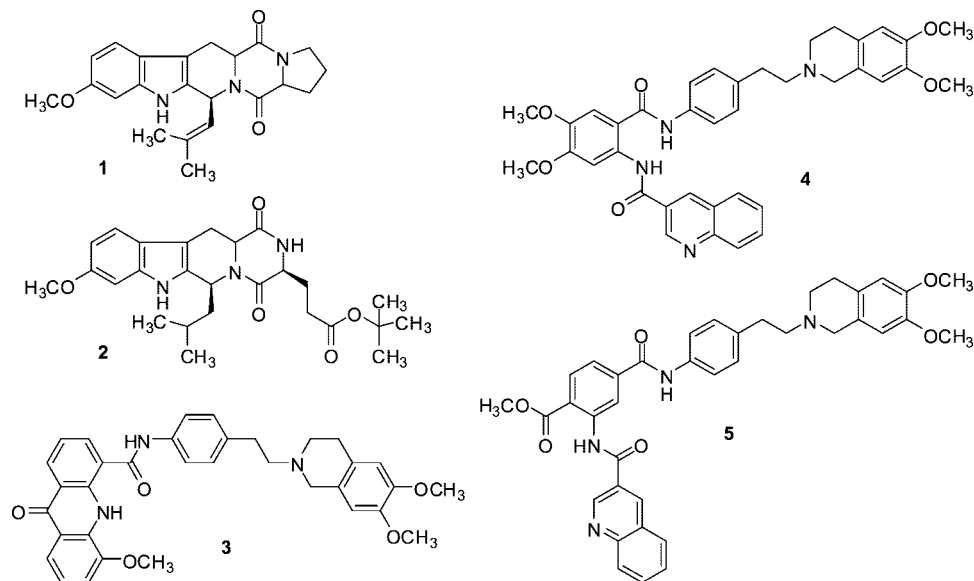


**Figure 1.** Structures of the ABCG2 modulators **1** (fumitremorgin C) and **2** (Ko143), the dual ABCB1/ABCG2 inhibitor **3** (elacridar), the ABCB1 inhibitor **4** (tariquidar), and the initial ABCG2 selective lead structure **5** derived from **4**.

result of their ABCG2-mediated drug resistance and slow proliferation, they are inefficient targets for classical cytostatic drugs.

Thus, in many respects, the potent and selective inhibition of ABCG2 might be a promising approach in cancer therapy. The reversal of the multidrug resistance mediated by ABCG2 and the specific targeting of the stem cell like side population are conceivable applications. Specific inhibition of ABCG2 in combination with a cytostatic, which is a substrate of ABCG2, might eradicate the tumor stem-cell population, provided that ABCG2 expression is actually a characteristic of these cells.

Another interesting strategy might be the coadministration of potent ABCG2 inhibitors with drugs that are substrates of the efflux pump to increase drug levels in the brain.<sup>18</sup> The latter has already been proven by the combination of the cytostatic paclitaxel (taxol A), an ABCB1 substrate, and the second generation ABCB1 inhibitor valspodar (6-[(2*S*,4*R*,6*E*)-4-Methyl-2-(methylamino)-3-oxo-6-octenoic acid]cyclosporin D),<sup>19</sup> as well as the third generation modulators, elacridar (GF120918) and tariquidar (XR 9576).<sup>20</sup> (**3** and **4**, Figure 1).

Because of the relatively recent discovery of the ABCG2 transporter, only a few ABCG2 inhibitors have been reported so far.<sup>21–25</sup> Fumitremorgin C (FTC, **1**, Figure 1), a diketopiperazine, isolated from the fermentation broth of *Aspergillus fumigatus*, was reported first.<sup>26</sup> However, its neurotoxicity precluded its use in in vivo experiments. The most potent ABCG2 inhibitor known so far is the FTC analogue **2** (Ko143).<sup>27</sup> Its low cytotoxicity made it promising for in vivo studies, and the bioavailability of orally administered topotecan ((4*S*)-10-[(dimethylamino)methyl]-4-ethyl-4,9-dihydroxy-1*H*-pyrano[3',4':6,7]indolizino[1,2-*b*]quinoline-3,14(4*H*,12*H*)-dione) could be increased by a combination with **2**.<sup>27</sup> Novobiocin (*N*-[7-[[3-*O*-(aminocarbonyl)-6-deoxy-5-*C*-methyl-4-*O*-methyl- $\beta$ -*L*-xylo-hexopyranosyl]oxy]-4-hydroxy-8-methyl-2-oxo-2*H*-1-benzopyran-3-yl]-4-hydroxy-3-(3-methyl-2-butenyl)benzamide), a coumermycin derivative and inhibitor of the prokaryotic enzyme gyrase, was also identified as an ABCG2 inhibitor. In cytotoxicity and flow cytometric assays, micromolar concentrations of novobiocin overcame ABCG2-mediated resistance to mitoxantrone (1,4-dihydroxy-5,8-bis[[2-[(2-hydroxyethyl)amino]ethyl]amino]anthracene-9,10-dione), topotecan, and the active

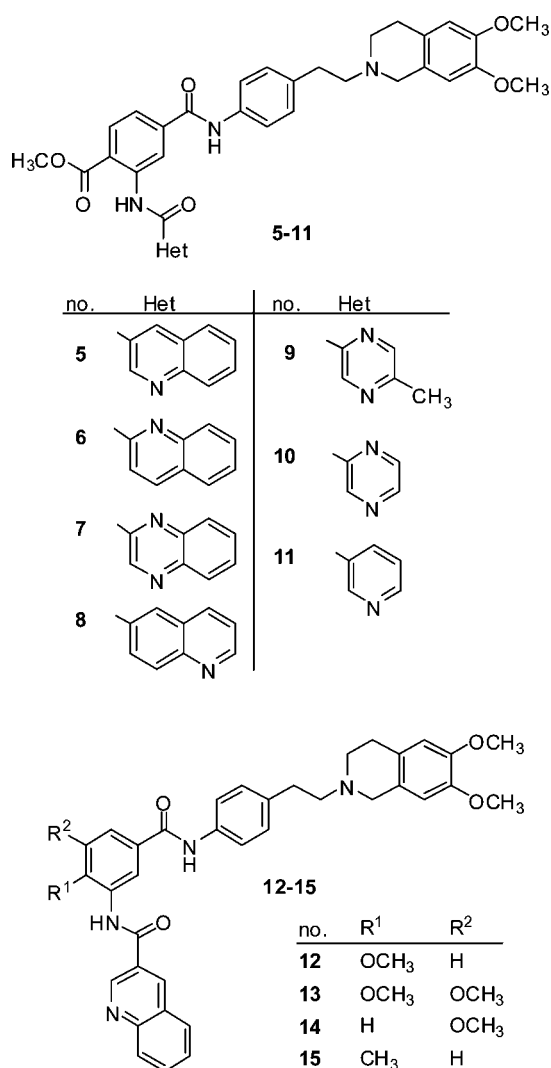
metabolite of irinotecan ([1,4'-bipiperidine]-1'-carboxylic acid (4*S*)-4,11-diethyl-3,4,12,14-tetrahydro-4-hydroxy-3,14-dioxo-1*H*-pyrano[3',4':6,7]indolizino[1,2-*b*]quinolin-9-yl ester).<sup>28</sup> Several ABCB1 inhibitors have also been reported to modulate ABCG2. It was demonstrated that **3**<sup>29</sup> acts as an ABCG2 inhibitor, as does (although with lower potency) the ABCB1 inhibitor **4**<sup>30</sup> and the analogue of **3** and **4**, WK-X-34 (*N*-[2-[[[4-[2-(3,4-dihydro-6,7-dimethoxy-2(1*H*)-isoquinolinyl)ethyl]-phenyl]amino]carbonyl]phenyl]-3,4-dimethoxybenzamide).<sup>31,32</sup>

A very recent structure–activity relationship study on analogues of **4** revealed preferential inhibition of ABCB1 compared to ABCG2. In these compounds the anthranilic acid portion was either acylated with different hetaroyl residues at the *o*-amino group or was replaced with (hetero)aromatic carboxylic acids.<sup>33</sup> During our work on tariquidar-like compounds as ABCB1 modulators,<sup>20,34,35</sup> we discovered that, surprisingly, minimal structural changes at the benzamide core of **4** (Figure 1) resulted in a potent and selective ABCG2 inhibitor (**5**, Figure 1 and Chart 1). On the basis of this finding, we prepared a series of new analogues that were characterized with respect to their activity and selectivity and are presented in this work.

## Results and Discussion

**Synthesis.** The design of the compounds described in this work was based on the serendipitous observation that compound **5** (Figure 1 and Chart 1) was only weakly active against ABCB1 but was found to be a potent ABCG2 inhibitor instead. Compared to the third generation ABCB1 inhibitor and anthranilic acid derivative **4**, the substitution pattern of carboxylic acid and amine functionalities at the central aromatic core of **5** was changed and the two methoxy groups were replaced by an ester group. Because this change apparently had a strong impact on the selectivity for ABCG2 versus ABCB1 (Table 1) we decided to prepare two small series of compounds in which either the 3-quinolinecarboxylic acid moiety was replaced by various heteroaromatic systems or the ester group was exchanged by methoxy and methyl substituents at different positions (Chart 1).

The general synthetic route for the title compounds (Scheme 1) comprises the formation of an amide bond between 3-nitrobenzoic acid analogues **16a–e** and the aromatic amine **17**,

**Chart 1.** Variation of the Lead Structure **5** (Subseries **5–11** and **12–15**)

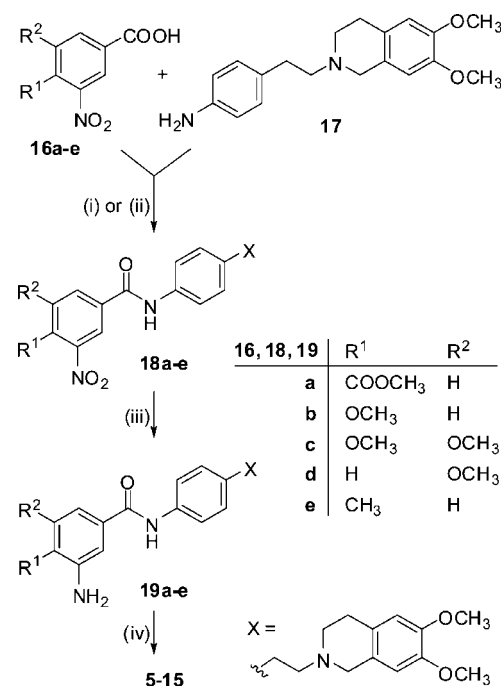
which was synthesized as described before.<sup>36</sup> Subsequent hydrogenation of the nitro group, followed by acylation of the resulting aromatic amines **19a–e** with different heteroaromatic carbonyl chlorides, yielded the compounds **5–15**.

**Inhibition of the ABC Transporters ABCG2, ABCB1, and ABCC2.** The synthesized modulators **5–15** and the reference compounds **1–4** were investigated for inhibition of ABCG2 and ABCB1 by flow cytometry in a mitoxantrone efflux assay and a calcein-AM efflux assay. In MCF-7/Topo cells, red fluorescent mitoxantrone is not accumulated but extruded by the ABCG2 transporter. Therefore, ABCG2 inhibitors can easily be recognized by the flow cytometric determination of intracellular mitoxantrone levels. Changes in the mitoxantrone efflux caused by different concentrations of the ABCG2 modulators can be measured by the relative fluorescence intensity of the cells. Similarly, in ABCB1 overexpressing KBv1 cells, the accumulation of calcein, a fluorescent substrate of ABCB1, can be quantified by flow cytometric analysis. In the presence of inhibitors of ABCB1, higher intracellular calcein levels lead to increased relative fluorescence intensities of the cells. The modulation of ABCC2 was investigated on ABCC2-overexpressing MDCK cells by incubation with chloromethylfluorescein-diacetate (CMFDA) in the absence and presence of increasing concentrations of test compounds. After intracellular formation of the ABCC2 substrate glutathione methylfluorescein

**Table 1.** Inhibition of ABCG2, ABCB1, and ABCC2 by Reference Compounds and the New Modulators **5–15** Determined in the Mitoxantrone (ABCG2), the Calcein-AM (ABCB1) Efflux, and the CMFDA Accumulation Assay (ABCC2)

compound	ABCG2 IC <sub>50</sub> [nM] <sup>a</sup>	ABCG2 maximal inhibitory effect [%] <sup>a,b</sup>	ABCB1 IC <sub>50</sub> [nM] <sup>c</sup>	ABCC2 IC <sub>50</sub> [nM]
<b>1</b> (fumitremorgin C)	> 11000	100	inactive <sup>d</sup>	inactive <sup>e</sup>
<b>2</b> (Ko143)	225 ± 33	82 ± 5	inactive <sup>d</sup>	> 50000
<b>3</b> (elacridar)	250 ± 45	46 ± 2	193 ± 18	inactive <sup>e</sup>
<b>4</b> (tariquidar)	916 ± 197	39 ± 3	223 ± 8	inactive <sup>e</sup>
<b>5</b>	119 ± 22	41 ± 3	9450 ± 417	inactive <sup>e</sup>
<b>6</b>	60 ± 10	56 ± 6	> 29000 <sup>f</sup>	> 20000
<b>7</b>	183 ± 50	55 ± 3	> 34000	nd
<b>8</b>	179 ± 35	25 ± 2	inactive <sup>d</sup>	nd
<b>9</b>	552 ± 125	44 ± 2	> 57000 <sup>f</sup>	> 20000
<b>10</b>	632 ± 222	38 ± 3	> 20000 <sup>f</sup>	> 50000
<b>11</b>	1015 ± 403	47 ± 4	> 14000 <sup>f</sup>	> 20000
<b>12</b>	317 ± 131	63 ± 7	> 6000 <sup>f</sup>	inactive <sup>e</sup>
<b>13</b>	858 ± 210	36 ± 3	> 17000	inactive <sup>e</sup>
<b>14</b>	977 ± 244	43 ± 6	> 15000	inactive <sup>e</sup>
<b>15</b>	1990 ± 355	52 <sup>f</sup>	> 15000 <sup>f</sup>	> 50000
MK571 <sup>g</sup>	nd	nd	nd	> 1000
LTC <sub>4</sub> <sup>h</sup>	nd	nd	nd	< 150

<sup>a</sup> Mean values ± SEM, calculated from two to three independent experiments. <sup>b</sup> Maximal inhibitory effects [%] are expressed as inhibition caused by the highest concentration of the compound tested (7 or 10 μM, respectively) relative to the inhibitory effect caused by 10 μM **1** (100% inhibition). <sup>c</sup> Mean values ± SEM, calculated from two to five independent experiments. <sup>d</sup> No effect up to a concentration of 10 μM; **1**: 0.8% inhibition at 10 μM, 22% inhibition at 100 μM; **2**: 1.6% inhibition at 10 μM. <sup>e</sup> No effect up to a concentration of 50 μM. <sup>f</sup> *N* = 1. <sup>g</sup> MK571: 3-(((3-(2-(7-chloroquinoline-2-yl)ethenyl)phenyl)((3-dimethylamino-3-oxopropyl)thio)ethyl)thio)propanoic acid. <sup>h</sup> LTC<sub>4</sub>: leukotriene C<sub>4</sub>. IC<sub>50</sub> values were calculated using SIGMA PLOT 9.0, four parameter logistic curve fitting; nd = not determined.

**Scheme 1.** General Synthetic Route for Compounds **5–15**<sup>a</sup>

<sup>a</sup> Reagents and conditions: (i) (1) SOCl<sub>2</sub>; (2) **17**, NEt<sub>3</sub>, CH<sub>2</sub>Cl<sub>2</sub>; (ii) HBTU, HOBT, DIPEA, **17**, CH<sub>2</sub>Cl<sub>2</sub>; (iii) H<sub>2</sub>, Pd/C, EtOAc/MeOH; (iv) HetC(O)Cl · HCl, NEt<sub>3</sub>, CH<sub>2</sub>Cl<sub>2</sub>/DMF.

(GSMF), the extent of intracellular fluorescence was monitored with a plate reader in a concentration-dependent manner.

To classify the new compounds with respect to their inhibitory potency against the targets ABCG2, ABCB1, and ABCC2 known modulators were investigated as references (Table 1).



Whereas **1** shows only an  $IC_{50}$  value in the micromolar range against ABCG2, its analogue **2** is a highly potent ABCG2 modulator with a maximal inhibitory effect of 82% referred to the control. Both compounds were inactive against the ABCB1 transporter, suggesting that the diketopiperazine partial structure confers some selectivity against ABCG2. However, the acridone carboxamide derivative **3**<sup>29</sup> strongly inhibits both transporters without a preference to one of the two targets, whereas **4** was about equipotent with **3** at ABCB1 but about four times less potent at ABCG2. Compounds **3** and **4** have the same *N*-substituent (dimethoxytetrahydroquinolinylethylphenyl) at acridonecarboxamide and benzamide, respectively. As shown very recently, the ABCG2 preference of acridonecarboxamides can be improved by replacing the amide substituent in **3** with methoxyphenylethyl residues.<sup>22</sup> Here we report that the preference for one of the ABC transporters depends on the core amide moiety in analogues of **4** with kept *N*-substituent.

Minimal structural changes at the benzamide core of **4** resulted in a change from ABCB1 to ABCG2 inhibition. The shift of the quinoline-3-carboxamido substituent from position **2** (**4**) to position **3** of the benzamide moiety (**13**) proved to be key to increase the selectivity for ABCG2 over ABCB1: whereas the moderate inhibition of ABCG2 was maintained (**13**:  $IC_{50}$  858 nM, **4**:  $IC_{50}$  916 nM), the inhibition of ABCB1 decreased by a factor of >75 ( $IC_{50}$  >17000 vs 223 nM for **13** and **4**, respectively). An additional step toward potent and selective ABCG2 inhibitors was the introduction of an ester instead of the methoxy groups. Comparing the methyl ester **5** with **4** and **13**, on one hand, the structural modification led to a strong increase in the modulatory potency against ABCG2, and on the other hand, the affinity against the original target ABCB1 was dramatically reduced. Similar to the lead structure **5**, the substances **6–11** were potent inhibitors of ABCG2 with up to 500-fold lower activity at ABCB1. None of the novel derivatives of **4** (up to a concentration of 50  $\mu$ M) exerted any inhibitory effect on ABCC2 (MRP2),

Obviously, the shift of the hetarylcarboxamido substituent from the 2- to the 3-position at the benzamide core of **4** dramatically changes the selectivity of the compounds for ABCG2 over ABCB1. All compounds with bicyclic hetarylcarboxamides in position **3** (**5–8**) were highly potent ABCG2 modulators ( $IC_{50}$  values within the range of the known ABCG2 inhibitor **2**) superior to the substances with monocyclic heteroaromatic moieties (**9–11**). The most potent inhibitor ( $IC_{50}$ :  $60 \pm 10$  nM) was obtained with a quinoline-2-carboxamido substituent (**6**). Although the methoxy-substituted compounds **12–14** showed some selectivity for ABCG2, these compounds were less potent than **5**. The decrease in activity was most pronounced with 5-methoxy substitution (**14**). Presumably, the carbonyl oxygen of the ester group in **5–11** contributes to the interaction with ABCG2. As the esters **5–11** may not be considered druglike due to susceptibility toward enzymatic hydrolysis, as an example, compound **5** was converted to the carboxylic acid. In the flow cytometric mitoxantrone efflux assay, the cleavage product turned out to be about 80 times less potent than the parent compound **5** as an inhibitor of ABCG2 (data not shown), i.e., higher potency resides in the esters.

As shown in Figure 2, the quinoline-3-carboxamide **5** and the structural isomer **6** were about as potent as **2**, the most potent ABCG2 modulator described so far. However, the maximum inhibition obtained by **2** was not reached. Although the lower efficacy compared to **1** appears to be characteristic of the new ABCG2 inhibitors related to **3**,<sup>22</sup> **4**, and **5**, the low water

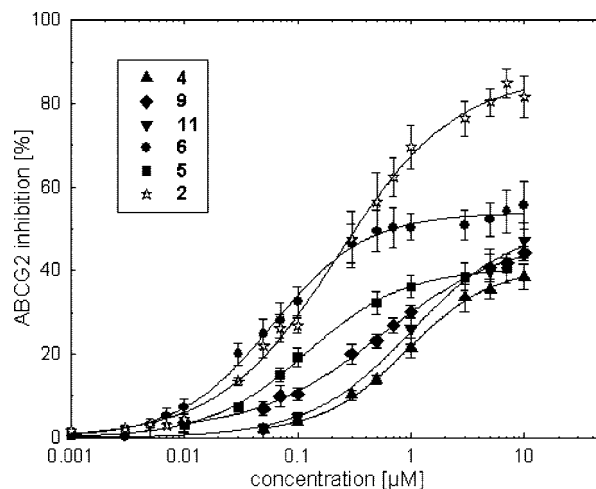


**Figure 2.** Concentration–response curves of ABCG2 inhibition by selected analogues of **4** (**5**, **6**, **9**, and **11**) and the reference compounds **2** (Ko143) and **4** (tariquidar).

solubility of the analogues of **4** presented in this work might contribute to this phenomenon. Stability investigations as well as the search for more stable bioisosteric replacements of the ester group and compounds with higher water solubility are the subjects of ongoing studies.

**Cytotoxicity and Reversal of Drug Resistance.** On the basis of the results of the mitoxantrone efflux assay, the ability of the two most potent modulators (**5** and **6**) to overcome multidrug resistance mediated by ABCG2 was investigated using a kinetic chemosensitivity assay. As a reference, in a further chemosensitivity assay, the known ABCG2-inhibitor **2** was used. For this purpose, ABCG2 positive topotecan-resistant MCF-7 breast cancer cells (MCF-7/Topo cells) were incubated with the inhibitors alone and in combination with topotecan at a nontoxic concentration. The results are shown in Figure 3.

Incubation of MCF-7/Topo breast cancer cells with **2** alone resulted in nontoxic effects up to a concentration of 500 nM. The combination of **2** at a concentration of 100 nM with topotecan at a nontoxic concentration of 100 nM yielded an overcome of the efflux pump mediated resistance. MCF-7/Topo breast cancer cells, which were incubated with the newly synthesized tariquidar analogue **6** alone, showed only a weak chemosensitivity up to concentrations of 500 nM (Figure 3C). However, compound **6** at a concentration of 100 nM combined with a nontoxic concentration of topotecan (100 nM) resulted in a strong cytostatic effect. The effective inhibition of ABCG2 led to a total reversal of the ABCG2 mediated topotecan resistance (Figure 3D). Surprisingly, at a concentration of 100 nM, compound **5** had a cytostatic effect against proliferating MCF-7/Topo cells (Figure 3E), which was only slightly enhanced by the combination with topotecan (Figure 3F). Chemosensitivity assays with proliferating ABCG2 negative U-373 MG glioblastoma cells indicate that the toxicity of **5** is independent from ABCG2 modulation. In addition, quiescent U-373 MG cells were not affected by **5**, indicating that the antiproliferative effect is cell cycle dependent (data not shown).

Specific modulators are desired as pharmacological tools for the functional analysis and characterization of the ABCG2 transporter as the mechanism of action, and the selection and binding of substrates is far from being understood. Some anticancer drugs, e.g., topotecan, are substrates of different ABC transporters. This might be one of the reasons why the reversal of MDR by inhibition of one of these proteins often fails in the clinics,<sup>37,38</sup> suggesting a potential therapeutic

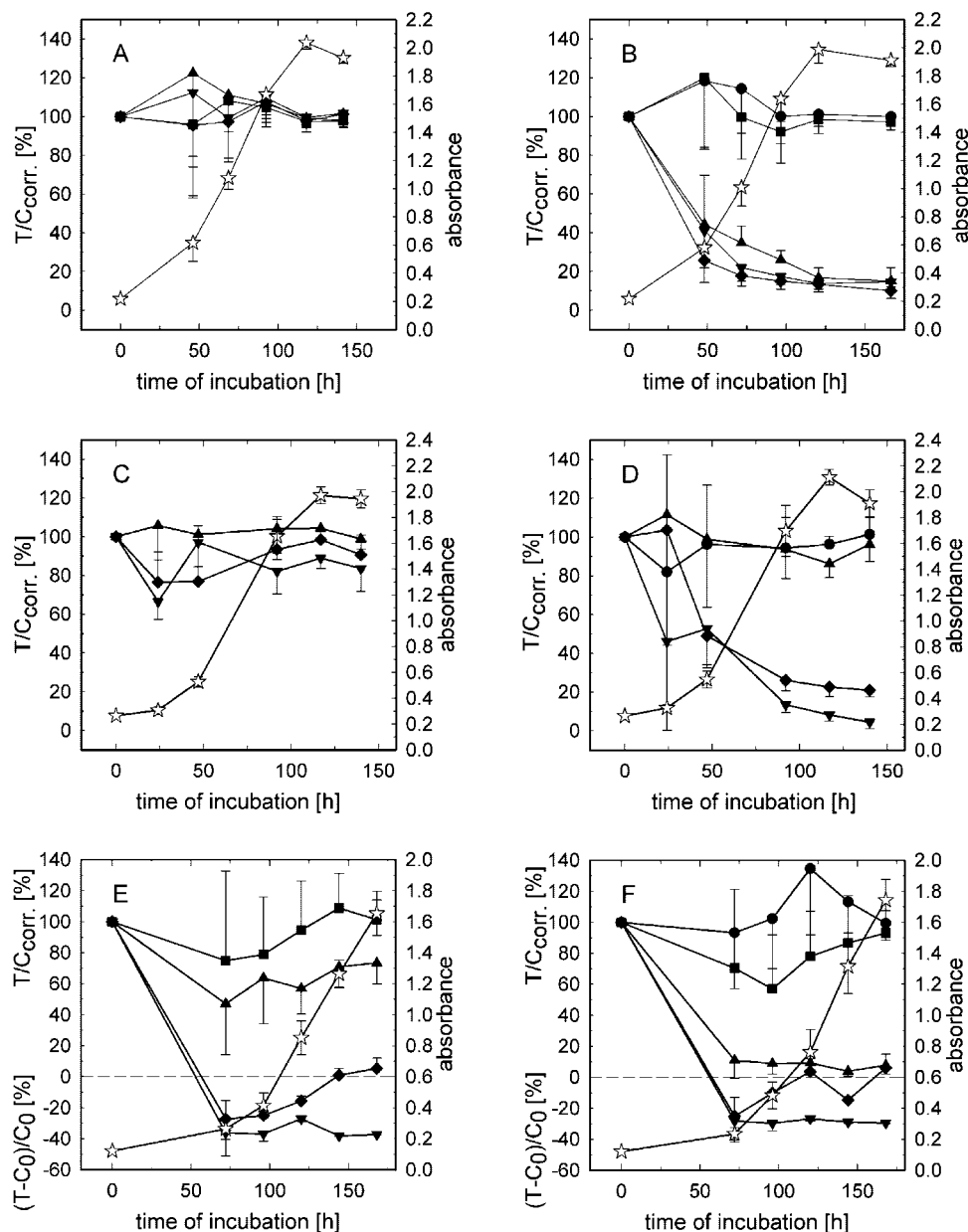


**Figure 3.** Effect of reference compound **2** alone (A) and in combination with 100 nM topotecan (B) on proliferating MCF-7/Topo cells (long-term drug exposure); vehicle (☆), 100 nM topotecan (●) and **2** at different concentrations: 10 nM (■), 50 nM (▲), 100 nM (▼), and 500 nM (◆). Effect of compound **6** alone (C) and in combination with 100 nM topotecan (D) on proliferating MCF-7/Topo cells (long-term drug exposure); vehicle (☆), 100 nM topotecan (●) and **6** at different concentrations: 10 nM (▲), 100 nM (◆), and 500 nM (▼). Effect of compound **5** alone (E) and in combination with topotecan (F) on proliferating MCF-7/Topo cells (permanent incubation with the test compounds); vehicle (☆), 100 nM topotecan (●) and **5** at different concentrations: 1 nM (■), 10 nM (▲), 100 nM (◆), and 500 nM (▼). Open stars represent the proliferation (absorbance, right ordinate in A–F) of the respective untreated cells (vehicle control). Thereby the A–F contain all the information necessary to reconstruct the individual growth curves of the treated cell populations (closed symbols) according to the equations in the Experimental Section (chemosensitivity assays).

value of dual inhibitors of ABC transporters.<sup>39</sup> Selective inhibition should be superior to dual ABCB1/ABCG2 inhibition, if the coadministered drug is preferentially transported by one specific efflux pump. Additionally, combination therapy could improve the pharmacokinetics of transported drugs, thereby increasing oral bioavailability,<sup>40</sup> plasma half-lives, and brain penetration.<sup>18,41</sup>

## Conclusions

Starting from the ABCB1 preferring dual ABCB1/ABCG2 modulator **4** (tariquidar), structural modifications at the benzamide core were performed. The synthesized compounds are

among the most potent and selective ABCG2 inhibitors known so far. Such compounds could be useful in combination with cytostatics, which are ABCG2 substrates, to overcome drug resistance of tumor cells, to modulate ABCG2 at the blood–brain barrier, and thereby to improve the outcome of cancer chemotherapy of malignant brain tumors. Kinetic chemosensitivity assays revealed two main effects of the new compounds. First, weakly toxic modulators such as compound **6** were able to reverse the ABCG2 mediated topotecan resistance in MCF-7/Topo breast cancer cells. Second, compound **5** showed additional cytotoxicity. The latter is an unexpected interesting aspect because ABCG2 modulators with intrinsic antiprolifera-

tive activity may offer a new chemotherapeutic approach addressing the tumor stem cell concept.<sup>42</sup>

## Experimental Section

**General.** Commercial reagents and starting materials were purchased from Aldrich, Fluka, or Acros and used without further purification. Flash chromatography was performed on silica gel (Merck silica gel Si 60 40–63  $\mu\text{m}$ ); products were detected by TLC on alumina plates coated with silica gel (Merck silica gel 60 F<sub>254</sub>, thickness 0.2 mm) and visualized by UV light ( $\lambda = 254 \text{ nm}$ ). Melting points were determined with a Büchi SMP 20 and are uncorrected. NMR spectra were recorded with Bruker Avance 300 (<sup>1</sup>H: 300.1 MHz; <sup>13</sup>C: 75.5 MHz;  $T = 300 \text{ K}$ ), Bruker Avance 400 (<sup>1</sup>H: 400.1 MHz; <sup>13</sup>C: 100.6 MHz;  $T = 300 \text{ K}$ ), and Bruker Avance 600 (<sup>1</sup>H: 600.1 MHz; <sup>13</sup>C: 150.1 MHz;  $T = 300 \text{ K}$ ) instruments. Chemical shifts are reported in  $\delta/\text{ppm}$  relative to external standards and coupling constants  $J$  are given in Hz. Abbreviations for the characterization of the signals: s = singlet, d = doublet, t = triplet, m = multiplet, bs = broad singlet, dd = double doublet. The relative numbers of protons is determined by integration. Error of reported values: chemical shift 0.01 ppm (<sup>1</sup>H NMR), 0.1 ppm (<sup>13</sup>C NMR), coupling constant 0.1 Hz. The used solvent for each spectrum is reported. Mass spectra were recorded with Finnigan MAT TSQ 7000 (ESI) and Finnigan MAT 90 (HRMS), IR spectra with a Bio-Rad FT-IR-FTS 155 spectrometer and UV/vis spectra with a Cary BIO 50 UV/vis/NIR spectrometer (Varian). For experimental details and analytical data for the intermediates **16d**, **18a–e**, **19a–e** and for the target compounds **5**, **7–15**, <sup>1</sup>H and <sup>13</sup>C NMR spectra and HPLC tracings of key target compounds cf. Supporting Information.

**General Procedure A for the Preparation of Carbonyl Chlorides.** The corresponding (hetero-) aromatic carboxylic acid was suspended in SOCl<sub>2</sub> (10–15 mL) and heated to reflux for two hours. Excess SOCl<sub>2</sub> was removed under reduced pressure, and the resulting white solid was dried under vacuum.

**General Procedures B and C for the Preparation of the Amide Bonds.** (B) The aromatic amine (**17**, **19a–d**) (1 equiv) and NEt<sub>3</sub> (3 equiv) were dissolved in CH<sub>2</sub>Cl<sub>2</sub>, and the aromatic carbonyl chloride (1.5 equiv) derived from the corresponding acid via general procedure A was added in small portions. The solution was stirred at room temperature for 24 h, diluted with CH<sub>2</sub>Cl<sub>2</sub>, washed with water and saturated aqueous solution of Na<sub>2</sub>CO<sub>3</sub> (3 $\times$ ), dried over MgSO<sub>4</sub>, and concentrated to give the crude product, which was purified by flash chromatography on silica gel or recrystallization. (C) The aromatic carboxylic acid (1.1 equiv), DIPEA (2 equiv), HOBt (1.2 equiv), and HBTU (1.2 equiv) were dissolved in CH<sub>2</sub>Cl<sub>2</sub> at 0 °C and stirred for 20 min. The amine (1 equiv) was added in small portions, and the solution was allowed to warm to room temperature and stirred for 24 h. The solution was diluted with CH<sub>2</sub>Cl<sub>2</sub>, washed with water (2 $\times$ ) and saturated aqueous solution of Na<sub>2</sub>CO<sub>3</sub> (3 $\times$ ), dried over MgSO<sub>4</sub>, and concentrated to give the crude product, which was purified by flash chromatography on silica gel.

**General Procedure D for the Reduction of the Nitro Group.** The corresponding nitro compound was dissolved in a mixture of ethyl acetate and methanol, palladium on activated charcoal (10% m/m) was added, and the solution was stirred under 5 bar H<sub>2</sub> atmosphere overnight. The catalyst was filtered off, and the solvents were removed to obtain the amines in quantitative yields.

**Methyl 4-((4-(2-(6,7-Dimethoxy-1,2,3,4-tetrahydroisoquinolin-2-yl)ethyl)phenyl)amino-carbonyl)-2-(quinoline-2-carboxylamino)benzoate (**6**).** The compound was synthesized following general procedure C and purified by flash chromatography on silica gel (5% MeOH/CHCl<sub>3</sub>,  $R_f = 0.36$ ) to obtain a pale-yellow solid (70 mg, 10%); mp = 176 °C (decomposition). <sup>1</sup>H NMR (300 MHz, CD<sub>2</sub>Cl<sub>2</sub>):  $\delta = 2.85\text{--}3.02$  (m, 8H, 4 CH<sub>2</sub>), 3.78 (s, 2H, NCH<sub>2</sub>), 3.84 (s, 3H, OCH<sub>3</sub>), 3.84 (s, 3H, OCH<sub>3</sub>), 4.07 (s, 3H, COOCH<sub>3</sub>), 6.54 (s, 1H, H–Ar), 6.60 (s, 1H, H–Ar), 7.24–7.27 (m, 2H, H–Ar, AA'BB'), 7.64–7.67 (m, 2H, H–Ar, AA'BB'), 7.62–7.67 (m, 1H, H–Ar), 7.69 (dd, <sup>3</sup> $J = 8.2 \text{ Hz}$ , <sup>4</sup> $J = 1.6 \text{ Hz}$ , 1H, H–Ar), 7.77–7.84 (m, 1H, H–Ar), 7.88–7.91 (m, 1H, H–Ar), 8.17 (d, <sup>3</sup> $J = 8.2 \text{ Hz}$ ,

1H, H–Ar), 8.28–8.36 (m, 3H, H–Ar), 8.34 (bs, 1H, CONH), 9.45 (d, <sup>4</sup> $J = 1.6 \text{ Hz}$ , 1H, H–Ar), 12.31 (bs, 1H, CONH). <sup>13</sup>C NMR (75 MHz, CDCl<sub>3</sub>/MeOD):  $\delta = 27.8$  (–), 32.9 (–), 50.7 (–), 52.8 (+), 55.0 (–), 55.9 (+), 56.0 (+), 59.4 (–), 109.4 (+), 111.3 (+), 117.9 (+), 118.7 (C<sub>quat</sub>), 118.8 (+), 120.8 (+), 122.5 (+), 123.3 (C<sub>quat</sub>), 124.8 (C<sub>quat</sub>), 125.4 (C<sub>quat</sub>), 127.7 (+), 128.5 (+), 129.3 (+), 129.4 (C<sub>quat</sub>), 130.2 (+), 130.4 (+), 131.9 (+), 136.1 (C<sub>quat</sub>), 137.8 (+), 140.1 (C<sub>quat</sub>), 140.8 (C<sub>quat</sub>), 146.6 (C<sub>quat</sub>), 147.5 (C<sub>quat</sub>), 147.8 (C<sub>quat</sub>), 149.5 (C<sub>quat</sub>), 163.9 (C<sub>quat</sub>), 164.8 (C<sub>quat</sub>), 167.4 (C<sub>quat</sub>). IR (KBr) [cm<sup>–1</sup>]:  $\nu = 3303, 2940, 2831, 1697, 1655, 1570, 1519$ . UV/vis (CHCl<sub>3</sub>)  $\lambda_{\text{max}}$  [nm] (lg  $\epsilon$ ): 309 (4.273), 289 (4.316), 245 (4.776). HRMS calcd. for C<sub>38</sub>H<sub>37</sub>N<sub>4</sub>O<sub>6</sub> [M<sup>+</sup>]: 645.2713; found: 645.2709.

**Drugs and Chemicals Used for Assays.** Mitoxantrone stocks were obtained by diluting Novantrone (Wyeth Pharma, Muenster, Germany) in 70% ethanol to a concentration of 2 mM. Test compounds were dissolved in DMSO (Merck, Darmstadt, Germany) at a concentration of 10 mM. Compound **1** (gift of Dr. Susan Bates, NIH) was also dissolved in DMSO and diluted to a concentration of 1 mM. A 10 mM stock solution of **2** in DMSO was kindly provided by Dr. A.H. Schinkel (Netherlands Cancer Institute). All stocks were stored at –20 °C. Topotecan stocks were prepared by diluting Hycamtin (GlaxoSmithKline, Munich, Germany) in 70% ethanol to a concentration of 0.1 mM and stored at 4 °C. Compound **4** (free base) was synthesized according to the literature with slight modifications.<sup>36</sup> Compound **3** was kindly provided by GlaxoSmithKline (Research Triangle Park, NC). Calcein-AM, purchased from Biotrend (Cologne, Germany), was dissolved in DMSO (Merck, Darmstadt, Germany) to achieve a final concentration of 1 mM. The aliquoted stock solutions were stored at –20 °C. The 1 mM stock solution of vinblastine (vinblastine sulfate, Sigma, Munich, Germany) was made in 70% ethanol.

**Cell Lines and Culture Condition.** MCF-7/Topo cells, an ABCG2 overexpressing subclone of MCF-7 breast cancer adenocarcinoma cells (ATTC HTB-22) were obtained by passaging the MCF-7 cells with increasing concentrations of topotecan in the culture medium to a maximum concentration of 0.55  $\mu\text{M}$ . Having reached the final concentration of topotecan, the cells were passaged after trypsinization using 0.05% trypsin/0.02% EDTA (PAA Laboratories, Pasching, Austria) every 3–5 days. The treated cells showed sufficient quantities of the ABCG2 transporter after three passages in Eagle's minimum essential medium (Sigma, Deisenhofen, Germany) containing L-glutamine, 2.2 g/L NaHCO<sub>3</sub> (Merck, Darmstadt, Germany), 0.11 g/L sodium pyruvate (Serva, Heidelberg, Germany), 5% fetal calf serum (Biochrom, Berlin, Germany), and topotecan at a concentration of 0.55  $\mu\text{M}$ .

KBv1 cells, an ABCB1 overexpressing subclone of KB cells (ATCC CCL-17), were maintained in Dulbecco's modified Eagle's medium (Sigma, Deisenhofen, Germany) supplemented with 10% FCS (Biochrom, Berlin, Germany) and 270 ng/mL vinblastine.

U-373 MG cells, an ABCB1 and ABCG2 nonexpressing human glioblastoma cell line, were cultured in Eagle's minimum essential medium (Sigma, Deisenhofen, Germany) containing L-glutamine, 2.2 g/L NaHCO<sub>3</sub> (Merck, Darmstadt, Germany), 0.11 g/L sodium pyruvate (Serva, Heidelberg, Germany), and 5% fetal calf serum (Biochrom, Berlin, Germany). All cells were cultured in a water-saturated atmosphere (95% air/5% CO<sub>2</sub>) at 37 °C in 75 cm<sup>2</sup> and 175 cm<sup>2</sup> culture flasks (NUNC, Wiesbaden, Germany and Greiner, Frickenhausen, Germany) respectively. Mycoplasma contamination was routinely monitored by polymerase chain reaction (Venor GeM, Minerva Biolabs GmbH, Berlin, Germany), and only mycoplasma free cultures were used for testing.

ABCC2 overexpressing MDCKII-MRP2 cells transfected with human ABCC2 were a kind gift from Prof. Dr. P. Borst (Netherlands Cancer Institute, Amsterdam). The cells were grown in Dulbecco's modified Eagle medium supplemented with 5% FCS (Biochrom, Berlin, Germany).

**Modulation of ABCG2 (BCRP, ABCP, MXR): Determination in the Flow Cytometric Mitoxantrone Efflux Assay.** The assay was essentially performed as described.<sup>35</sup> Briefly, 3–5 days after passaging, the ABCG2 overexpressing MCF-7/Topo cells were trypsinized and resuspended in culture medium at 25 °C. After



adjusting the cells to a number of  $1 \times 10^6$  per mL with culture medium, mitoxantrone was added to the cell suspension to achieve a concentration of 20  $\mu\text{M}$ . Different concentrations of the test compound, solvent, and **1** (final concentration 10  $\mu\text{M}$ ) were added, respectively. The cell suspensions were vortexed and incubated for 30 min at 37 °C/5%  $\text{CO}_2$  to allow maximal mitoxantrone uptake into the cells. After one washing step with 0.8 mL of ice-cold PBS, the cells of the sample containing **1** were resuspended in 0.5 mL of PBS and placed on ice in the dark until the measurement to avoid mitoxantrone efflux (determination of the 100% mitoxantrone uptake). All other samples were resuspended in 1 mL of drug-free culture medium and incubated for 1 h at 37 °C/5%  $\text{CO}_2$  in which an equilibrium of mitoxantrone could be reached between the cytoplasm and the surrounding medium. Subsequently, after the medium was removed by centrifugation, the cell pellets were rinsed once with 0.8 mL of ice-cold PBS and finally resuspended in 0.5 mL of PBS for the flow cytometry. A FACS calibur (Becton Dickinson, Heidelberg, Germany) was used to analyze the fluorescence intensity of the cells. Mitoxantrone accumulation in the cells was monitored by using an excitation wavelength of 635 nm, whereas emission was detected at a wavelength of 661 nm. A minimum of 20000 events was collected per sample, and the events were gated according to forward scatter and sideward scatter to exclude clumps and debris. Analysis of the raw data was performed with the WinMDI 2.8 software. The geometric means were calculated from the fluorescence intensity histogram and related to the controls. Afterward, the mean values of 3 independent measurements were plotted against the concentration of the test compounds. Addition of increasing concentrations of the modulator led to sigmoidal concentration response curves.  $\text{IC}_{50}$  values were calculated using SIGMA PLOT 9.0, four parameter logistic curve fitting. Errors were calculated as standard error of the mean.

**Modulation of ABCB1 (p-gp): Determination in the Flow Cytometric Calcein-AM Assay.** The assay was performed as described.<sup>43</sup>

**Modulation of ABCC2 (MRP2): Determination in the CM-FDA Assay.** Cells were kept in culture in 24-well plates. They were washed twice with Krebs–Ringer buffer (KRB) at 37 °C prior to experiments and then incubated with 1  $\mu\text{M}$  CMFDA in the absence or the presence of the test compounds at increasing concentrations. Typically, the modulators were dissolved in DMSO. Control experiments confirmed that the cell monolayers tolerated up to 1% DMSO in the incubation medium without functional impairment. All monolayers were incubated for 90 min at 37 °C and under constant circular shaking at 50 rpm. Subsequently, the culture plates were placed on ice, medium in the apical compartment was removed, and the cells were washed twice with ice-cold KRB. The cells were lysed by incubation with 200  $\mu\text{L}$  of 1% Triton X-100 in KRB for 30 min under constant shaking. Finally, the culture plates were subjected to fluorescence quantification in a plate reader (Tecan Safire XFLUOR4, Tecan Safire, Crailsheim, Germany) with filter settings of  $\lambda_{\text{ex}}$  of 485 nm and  $\lambda_{\text{em}}$  of 516 nm. The extent of transport inhibition in presence of ABCC2 modulators was calculated from fluorescence intensities using the software GraphPad Prism (GraphPad Software, Inc., San Diego, CA).

**Chemosensitivity Assays.** The assays were performed as described previously.<sup>44</sup> In brief: tumor cell suspensions (100  $\mu\text{L}$ /well) were seeded into 96-well flat bottomed microtiteration plates (Greiner, Frickenhausen, Germany) at a density of ca. 15 cells/microscopic field (magnification 320-fold). After 2–3 days, the culture medium was removed by suction and replaced by fresh medium (200  $\mu\text{L}$ /well) containing varying drug concentrations or vehicle. Drugs were added as 1000-fold concentrated feed solutions. On every plate, 16 wells served as controls and 16 wells were used per drug concentration. After various times of incubation, the cells were fixed with glutaraldehyde (Merck, Darmstadt, Germany) and stored in a refrigerator. At the end of the experiment, all plates were processed simultaneously (staining with 0.02% aqueous crystal violet (SERVA, Heidelberg, Germany) solution (100  $\mu\text{L}$ /well)). Excess dye was removed by rinsing the trays with water for 20 min. The stain bound by the cells was redissolved in 70% ethanol

(180  $\mu\text{L}$ /well) while shaking the microplates for about 3 h. Absorbance (a parameter proportional to cell mass) was measured at 578 nm using a BIOTEK 309 Autoreader (TECNOMARA, Fernwald, Germany).

Drug effects were expressed as corrected T/C-values for each group according to

$$T/C_{\text{corr}} = \frac{T - C_0}{C - C_0} \times 100 [\%]$$

where  $T$  is the mean absorbance of the treated cells,  $C$  the mean absorbance of the controls, and  $C_0$  the mean absorbance of the cells at the time ( $t = 0$ ) when drug was added. When the absorbance of treated cells  $T$  is less than that of the culture at  $t = 0$  ( $C_0$ ), the extent of cell killing was calculated as

$$\text{cytotoxic effect } [\%] = \frac{C_0 - T}{C_0} \times 100$$

For assays performed on quiescent U-373 MG cells, a high sowings density was chosen in order to observe as much as possible the effects of the compounds against resting cells. To detect maximum cytotoxic effect rotenone, an ubiquinone reductase inhibitor, blocking ATP synthesis, served as positive control.

**Acknowledgment.** This work was supported by the Graduate Training Program (Graduiertenkolleg) GRK 760, “Medicinal Chemistry: Molecular Recognition—Ligand—Receptor Interactions”, of the Deutsche Forschungsgemeinschaft and the Fonds der Chemischen Industrie. M.E. thanks the Elitenetzwerk Bayern for a graduate fellowship. We thank Carolin Fischer for the synthesis of the carboxylic acid corresponding to ester **5**, Dr. A. H. Schinkel, Netherlands Cancer Institute (Amsterdam) for kindly providing **2** (Ko143), Dr. Susan Bates from the NIH (Bethesda, MD) for the reference compound **1** (fumitremorgin C), and Dr. P. Borst (Netherlands Cancer Institute, Amsterdam) for providing the ABCC2 overexpressing MDCKII-MRP2 cells.

**Supporting Information Available:** Experimental details and analytical data for the intermediates **16d**, **18a–e**, **19a–e** and for the target compounds **5**, **7–15**,  $^1\text{H}$ - and  $^{13}\text{C}$  NMR spectra and HPLC analysis including tracings of key target compounds. This material is available free of charge via the Internet at <http://pubs.acs.org>.

## References

- (1) Borst, P.; Kool, M.; Evers, R. Do cMOAT (MRP2), other MRP homologues, and LRP play a role in MDR? *Semin. Cancer Biol.* **1997**, *8*, 205–213.
- (2) Kuwano, M.; Toh, S.; Uchiumi, T.; Takano, H.; Kohno, K.; Wada, M. Multidrug resistance-associated protein subfamily transporters and drug resistance. *Anti-Cancer Drug Des.* **1999**, *14*, 123–131.
- (3) Cervenak, J.; Andrikovics, H.; Ozvegy-Laczka, C.; Tordai, A.; Nemet, K.; Varadi, A.; Sarkadi, B. The role of the human ABCG2 multidrug transporter and its variants in cancer therapy and toxicology. *Cancer Lett.* **2006**, *234*, 62–72.
- (4) Dean, M.; Allikmets, R. Complete Characterization of the Human ABC Gene Family. *J. Bioenerg. Biomembr.* **2001**, *33*, 475–479.
- (5) Robey, R.; Polgar, O.; Deeken, J.; To, K.; Bates, S. ABCG2: determining its relevance in clinical drug resistance. *Cancer Metastasis Rev.* **2007**, *26*, 39–57.
- (6) Staud, F.; Vackova, Z.; Pospechova, K.; Pavek, P.; Ceckova, M.; Libra, A.; Cygalova, L.; Nachtigal, P.; Fendrich, Z. Expression and Transport Activity of Breast Cancer Resistance Protein (Bcrp/Abcg2) in Dually Perfused Rat Placenta and HRP-1 Cell Line. *J. Pharmacol. Exp. Ther.* **2006**, *319*, 53–62.
- (7) Régina, A.; Demeule, M.; Laplante, A.; Jodoin, J.; Dagenais, C.; Berthelet, F.; Moghrabi, A.; Béliveau, R. Multidrug Resistance in Brain Tumors: Roles of the Blood–Brain Barrier. *Cancer Metastasis Rev.* **2001**, *20*, 13–25.
- (8) Leonard, G. D.; Fojo, T.; Bates, S. E. The Role of ABC Transporters in Clinical Practice. *Oncologist* **2003**, *8*, 411–424.
- (9) Sheps, J.; Ling, V. Preface: the concept and consequences of multidrug resistance. *Pflügers Arch. Eur. J. Physiol.* **2007**, *453*, 545–553.

- (10) Doyle, L. A.; Yang, W.; Abruzzo, L. V.; Krogmann, T.; Gao, Y.; Rishi, A. K.; Ross, D. D. A multidrug resistance transporter from human MCF-7 breast cancer cells. *Proc. Natl. Acad. Sci. U.S.A.* **1998**, *95*, 15665–15670.
- (11) Allikmets, R.; Schriml, L. M.; Hutchinson, A.; Romano-Spica, V.; Dean, M. A Human Placenta-Specific ATP-Binding Cassette Gene (ABCP) on Chromosome 4q22 That Is Involved in Multidrug Resistance. *Cancer Res.* **1998**, *58*, 5337–5339.
- (12) Bunting, K. D. ABC Transporters as Phenotypic Markers and Functional Regulators of Stem Cells. *Stem Cells* **2002**, *20*, 11–20.
- (13) Jonker, J. W.; Freeman, J.; Bolscher, E.; Musters, S.; Alvi, A. J.; Titley, I.; Schinkel, A. H.; Dale, T. C. Contribution of the ABC Transporters Bcrp1 and Mdr1a/1b to the Side Population Phenotype in Mammary Gland and Bone Marrow of Mice. *Stem Cells* **2005**, *23*, 1059–1065.
- (14) Sung, J. M.; Cho, H. J.; Yi, H.; Lee, C. H.; Kim, H. S.; Kim, D. K.; Abd El-Aty, A. M.; Kim, J. S.; Landowski, C. P.; Hediger, M. A.; Shin, H. C. Characterization of a stem cell population in lung cancer A549 cells. *Biochem. Biophys. Res. Commun.* **2008**, *371*, 163–167.
- (15) Kondo, T.; Setoguchi, T.; Taga, T. Persistence of a small subpopulation of cancer stem-like cells in the C6 glioma cell line. *Proc. Natl. Acad. Sci. U.S.A.* **2004**, *101*, 781–786.
- (16) Hirschmann-Jax, C.; Foster, A. E.; Wulf, G. G.; Nuchtern, J. G.; Jax, T. W.; Gobel, U.; Goodell, M. A.; Brenner, M. K. A distinct “side population” of cells with high drug efflux capacity in human tumor cells. *Proc. Natl. Acad. Sci. U.S.A.* **2004**, *101*, 14228–14233.
- (17) Haraguchi, N.; Utsunomiya, T.; Inoue, H.; Tanaka, F.; Mimori, K.; Barnard, G. F.; Mori, M. Characterization of a Side Population of Cancer Cells from Human Gastrointestinal System. *Stem Cells* **2006**, *24*, 506–513.
- (18) Breedveld, P.; Beijnen, J. H.; Schellens, J. H. M. Use of *p*-glycoprotein and BCRP inhibitors to improve oral bioavailability and CNS penetration of anticancer drugs. *Trends Pharmacol. Sci.* **2006**, *27*, 17–24.
- (19) Fellner, S.; Bauer, B.; Müller, D. S.; Schaffrik, M.; Fankhänel, M.; Spruss, T.; Bernhardt, G.; Gräff, C.; Färber, L.; Gschaidmeier, H.; Buschauer, A.; Fricker, G. Transport of paclitaxel (Taxol) across the blood–brain barrier in vitro and in vivo. *J. Clin. Invest.* **2002**, *110*, 1309–1318.
- (20) Hubensack, M.; Müller, C.; Höcherl, P.; Fellner, S.; Spruss, T.; Bernhardt, G.; Buschauer, A. Effect of the ABCB1 modulators elacridar and tariquidar on the distribution of paclitaxel in nude mice. *J. Cancer Res. Clin. Oncol.* **2008**, *134*, 597–607.
- (21) Ahmed-Belkacem, A.; Pozza, A.; Macalou, S.; Perez-Victoria, J. M.; Boumendjel, A.; Di Pietro, A. Inhibitors of cancer cell multidrug resistance mediated by breast cancer resistance protein (BCRP/ABCG2). *Anticancer Drugs* **2006**, *17*, 239–243.
- (22) Boumendjel, A.; Macalou, S.; Ahmed-Belkacem, A.; Blanc, M.; Di Pietro, A. Acridone derivatives: design, synthesis, and inhibition of breast cancer resistance protein ABCG2. *Bioorg. Med. Chem.* **2007**, *15*, 2892–2897.
- (23) Han, Y.; Riwan, M.; Go, M. L.; Ee, P. L. R. Modulation of breast cancer resistance protein (BCRP/ABCG2) by non-basic chalcone analogues. *Eur. J. Pharm. Sci.* **2008**, *35*, 30–41.
- (24) Liu, X. L.; Tee, H. W.; Go, M. L. Functionalized chalcones as selective inhibitors of *p*-glycoprotein and breast cancer resistance protein. *Bioorg. Med. Chem.* **2008**, *16*, 171–180.
- (25) Jain, H. D.; Zhang, C.; Zhou, S.; Zhou, H.; Ma, J.; Liu, X.; Liao, X.; Deveau, A. M.; Dieckhaus, C. M.; Johnson, M. A.; Smith, K. S.; Macdonald, T. L.; Kakeya, H.; Osada, H.; Cook, J. M. Synthesis and structure–activity relationship studies on tryprostatin A, an inhibitor of breast cancer resistance protein. *Bioorg. Med. Chem.* **2008**, *16*, 4626–4651.
- (26) Rabindran, S. K.; Ross, D. D.; Doyle, L. A.; Yang, W.; Greenberger, L. M. Fumitremorgin C Reverses Multidrug Resistance in Cells Transfected with the Breast Cancer Resistance Protein. *Cancer Res.* **2000**, *60*, 47–50.
- (27) Allen, J. D.; van Loevezijn, A.; Lakhai, J. M.; van der Valk, M.; van Tellingen, O.; Reid, G.; Schellens, J. H. M.; Koomen, G.-J.; Schinkel, A. H. Potent and Specific Inhibition of the Breast Cancer Resistance Protein Multidrug Transporter in Vitro and in Mouse Intestine by a Novel Analogue of Fumitremorgin C. *Mol. Cancer Ther.* **2002**, *1*, 417–425.
- (28) Shiozawa, K.; Oka, M.; Soda, H.; Yoshikawa, M.; Ikegami, Y.; Tsurutani, J.; Nakatomi, K.; Nakamura, Y.; Doi, S.; Kitazaki, T.; Mizuta, Y.; Murase, K.; Yoshida, H.; Ross, D. D.; Kohno, S. Reversal of breast cancer resistance protein (BCRP/ABCG2)-mediated drug resistance by novobiocin, a coumermycin antibiotic. *Int. J. Cancer* **2004**, *108*, 146–151.
- (29) de Bruin, M.; Miyake, K.; Litman, T.; Robey, R.; Bates, S. E. Reversal of resistance by GF120918 in cell lines expressing the ABC half-transporter, MXR. *Cancer Lett.* **1999**, *146*, 117–126.
- (30) Robey, R. W.; Steadman, K.; Polgar, O.; Morisaki, K.; Blayney, M.; Mistry, P.; Bates, S. E. Pheophorbide A Is a Specific Probe for ABCG2 Function and Inhibition. *Cancer Res.* **2004**, *64*, 1242–1246.
- (31) Jekerle, V.; Klinkhammer, W.; Scollard, D. A.; Breitbach, K.; Reilly, R. M.; Piquette-Miller, M.; Wiese, M. In vitro and in vivo evaluation of WK-X-34, a novel inhibitor of *p*-glycoprotein and BCRP, using radio imaging techniques. *Int. J. Cancer* **2006**, *119*, 414–422.
- (32) Jekerle, V.; Klinkhammer, W.; Reilly, R. M.; Piquette-Miller, M.; Wiese, M. Novel tetrahydroisoquinolin-ethyl-phenylamine based multidrug resistance inhibitors with broad-spectrum modulating properties. *Cancer Chemother. Pharmacol.* **2007**, *59*, 61–69.
- (33) Pick, A.; Müller, H.; Wiese, M. Structure–activity relationships of new inhibitors of breast cancer resistance protein (ABCG2). *Bioorg. Med. Chem.* **2008**, *16*, 8224–8236.
- (34) Egger, M.; Li, X.; Müller, C.; Bernhardt, G.; Buschauer, A.; König, B. Tariquidar Analogues: Synthesis by Cu<sup>I</sup>-Catalysed N/O-Aryl Coupling and Inhibitory Activity against the ABCB1 transporter. *Eur. J. Org. Chem.* **2007**, *264*, 3–2649.
- (35) Müller, C. New approaches to the therapy of glioblastoma: investigations on RNA interference, kinesin Eg5 and ABCB1/ABCG2 inhibition. Doctoral Thesis. University of Regensburg: Regensburg, Germany, 2007; <http://www.opus-bayern.de/uni-regensburg/volltexte/2007/816/>.
- (36) Hubensack, M. Approaches to overcome the blood brain barrier in the chemotherapy of primary and secondary brain tumors: modulation of P-glycoprotein 170 and targeting of the transferrin receptor. Doctoral Thesis. University of Regensburg: Regensburg, Germany, 2005; <http://www.opus-bayern.de/uni-regensburg/volltexte/2005/471/>.
- (37) Staud, F.; Pavek, P. Breast cancer resistance protein (BCRP/ABCG2). *Int. J. Biochem. Cell Biol.* **2005**, *37*, 720–725.
- (38) Litman, T.; Brangi, M.; Hudson, E.; Fetsch, P.; Abati, A.; Ross, D. D.; Miyake, K.; Resau, J. H.; Bates, S. E. The multidrug-resistant phenotype associated with overexpression of the new ABC half-transporter, MXR (ABCG2). *J. Cell Sci.* **2000**, *113*, 2011–2021.
- (39) de Vries, N. A.; Zhao, J.; Kroon, E.; Buckle, T.; Beijnen, J. H.; van Tellingen, O. P-glycoprotein and breast cancer resistance protein: two dominant transporters working together in limiting the brain penetration of topotecan. *Clin. Cancer Res.* **2007**, *13*, 6440–6449.
- (40) Su, Y.; Hu, P.; Lee, S. H.; Sinko, P. J. Using novobiocin as a specific inhibitor of breast cancer resistant protein to assess the role of transporter in the absorption and disposition of topotecan. *J. Pharm. Pharm. Sci.* **2007**, *10*, 519–536.
- (41) Zhuang, Y.; Fraga, C. H.; Hubbard, K. E.; Hagedorn, N.; Panetta, J. C.; Waters, C. M.; Stewart, C. F. Topotecan central nervous system penetration is altered by a tyrosine kinase inhibitor. *Cancer Res.* **2006**, *66*, 11305–11313.
- (42) Reya, T.; Morrison, S. J.; Clarke, M. F.; Weissman, I. L. Stem cells, cancer and cancer stem cells. *Nature* **2001**, *414*, 105–111.
- (43) Müller, C.; Gross, D.; Sarli, V.; Gartner, M.; Giannis, A.; Bernhardt, G.; Buschauer, A. Inhibitors of kinesin Eg5: antiproliferative activity of monastrol analogues against human glioblastoma cells. *Cancer Chemother. Pharmacol.* **2007**, *59*, 157–164.
- (44) Bernhardt, G.; Reile, H.; Birnböck, H.; Spruss, T.; Schönenberger, H. Standardized kinetic microassay to quantify differential chemosensitivity on the basis of proliferative activity. *J. Cancer Res. Clin. Oncol.* **1992**, *118*, 35–41.

JM8013822